

Purdue University

Purdue e-Pubs

International Refrigeration and Air Conditioning
Conference

School of Mechanical Engineering

2022

Performance Analysis of an R410A Air-to-Water Heat Pump for Different Fan and Compressor Speed Combinations

Ignacio Ortega

Jaime Sieres

Fernando Cerdeira

José M. Santos

Estrella Álvarez

Follow this and additional works at: <https://docs.lib.purdue.edu/iracc>

Ortega, Ignacio; Sieres, Jaime; Cerdeira, Fernando; Santos, José M.; and Álvarez, Estrella, "Performance Analysis of an R410A Air-to-Water Heat Pump for Different Fan and Compressor Speed Combinations" (2022). *International Refrigeration and Air Conditioning Conference*. Paper 2316.
<https://docs.lib.purdue.edu/iracc/2316>

This document has been made available through Purdue e-Pubs, a service of the Purdue University Libraries. Please contact epubs@purdue.edu for additional information. Complete proceedings may be acquired in print and on CD-ROM directly from the Ray W. Herrick Laboratories at <https://engineering.purdue.edu/Herrick/Events/orderlit.html>

Performance Analysis of an R410A Air-to-Water Heat Pump for Different Fan and Compressor Speed Combinations

Ignacio ORTEGA¹, Jaime SIERES^{1*}, Fernando CERDEIRA¹, José M. SANTOS¹, Estrella ÁLVAREZ²

¹Área de Máquinas y Motores Térmicos, Escuela de Ingeniería Industrial, University of Vigo, Campus Lagoas-Marcosende 9, 36310 Vigo, Spain
iortega@uvigo.es, jsieres@uvigo.es, nano@uvigo.es, josanna@uvigo.es

²Chemical Engineering Department, Escuela de Ingeniería Industrial, University of Vigo, Campus Lagoas-Marcosende 9, 36310 Vigo, Spain
ealvarez@uvigo.es

* Corresponding Author

ABSTRACT

In this paper, the performance of an air-to-water heat pump with R410A is studied. The unit works following a flash tank vapor injection cycle (using a vapor-injected compressor). It also includes a four-way reversing valve, electronic expansion valves, a plate heat exchanger as the indoor heat exchanger, and a coil with wavy fins as the outdoor heat exchanger.

In the residential heat pump sector energy efficiency policies have boosted the development of efficient units that include variable speed compressor or electronic expansion valves (EEV) as some of their technological improvements. Though the fan power consumption may not be relevant at the nominal conditions (high compressor speeds), it may turn to be significant at partial load. Then, in order to obtain high SCOP/SEER values, the unit's fan speed should be controlled properly.

Experimental results for typical operating conditions of air-to-water heat pumps (EN 14511-2, 2018) in the cooling mode of operation are presented and discussed for different fan and compressor speed combinations. From the experimental measurements, parameters such as the EER, the cooling power or the compressor and fan electric power consumptions are obtained and analyzed. Results show that an optimum fan speed that maximizes the EES of the unit can be found for different compressor speed values. The optimum fan speed decreases when the compressor speed decreases. For the range of conditions tested in this work, the effect of the fan speed control on the EER can represent an improvement of up to 6%.

1. INTRODUCTION

In the last decade, worldwide regulations and policies have been approved with the final objective of reducing emissions that contribute to global warming. In the EU this has led to a set of proposals which affect the heating and cooling energy sector and will have a direct impact on the development and market penetration of heat pumps and refrigeration units.

One of these proposals is related with energy efficiency policies. The directive 2018/2002/EU on energy efficiency establishes a common framework of measures to ensure EU 2030 targets for final and primary energy consumption reductions. Heat pumps are highly efficient equipment for heating applications, so the replacement of the current heating equipment in the building stock (mainly based on fossil-fuels) by heat pumps could contribute to a great reduction of the primary energy consumption in buildings. Additionally, in the heat pump sector, energy efficiency policies have boosted the development of units that include variable speed compressor or electronic expansion valves (EEV) as some of their technological improvements, which have higher seasonal efficiency values than the traditional constant compressor speed (on/off operation) units.

Today the residential and commercial air-conditioning and heat pump market relies mainly on HFCs refrigerants (UNEP, 2019). A significant portion of residential air conditioners and heat pumps are based on refrigerant R410A for both ground and air-source units. Both technologies have been widely adopted worldwide for space heating and cooling as well as for domestic hot water (DHW) production in residential buildings. Due to the lower cost and ease of installation of air-source heat pumps (ASHP), air is and will remain the dominant energy source for heat pumps (EHPA, 2020).

ASHP are widely adopted in residential buildings to supply the cooling/heating and DHW needs. However, in cold climates their performance deteriorates since as the ambient temperature decreases the heat output diminishes, the compressor discharge temperature increases and the COP decreases (Bertsch and Groll, 2008). To improve the ASHP behavior at low temperatures, different cycle modifications have been proposed (Bertsch and Groll, 2008). One of such possible modifications is the use of an enhanced vapor injection (EVI) cycle. With this technique, vapor is injected at the intermediate stage of the compressor (Shuxue et al., 2013). When compared with one stage cycles, the main difference of the EVI cycle is that its efficiency is not only linked with the temperatures of the source and sink but it also depends on how the vapor injection is done (Redón et al., 2014).

The flash tank cycle and the internal heat exchanger cycle are two of the major vapor injection configurations (Wang and Li, 2019). Compared to the internal heat exchanger configuration, the flash tank configuration has the merit of a lower cost (Wang and Li, 2019). The refrigerant circuitry of the flash tank configuration is simpler and seems more appropriate for an invertible heat pump equipped with a four-way valve. Many previous studies about flash tank EVI cycles are found in the opening literature related with the effect of the vapor injection state on the system performance (Winandy and Lebrun, 2002; Xu et al., 2011; Navarro et al., 2013)

This paper is focused on an air-to-water heat pump using refrigerant R410A. The unit works following a flash tank EVI cycle (using a vapor-injected compressor). It also includes a four-way reversing valve, electronic expansion valves, a plate heat exchanger as the indoor heat exchanger, and a coil with wavy fins as the outdoor heat exchanger.

The heat pump unit includes a variable speed compressor. In this type of systems, the compressor speed is continuously controlled in order to meet the building or space cooling thermal load variations. Though the fan power consumption may not be relevant at the nominal conditions (high compressor speeds), it may turn to be significant at partial load. The main objective of this work is to evaluate the effect of the fan speed at different compressor speed conditions (cooling power requirements). Experimental results for typical operating conditions of air-to-water heat pumps (EN 14511-2, 2018) in the cooling mode of operation are presented and discussed for different fan and compressor speed combinations. From the experimental measurements, parameters such as the EER, the cooling power or the compressor and fan electric power consumptions are obtained and analyzed.

2. EXPERIMENTAL SET-UP

The main component of the experimental set-up is an air-to-water to water heat pump, which can work under the heating or cooling modes of operation. The refrigerant used is R410A.

Figure 1 shows a schematic representation of the heat pump in the cooling mode of operation. The heat pump has a variable-speed scroll type compressor with vapor injection. The indoor heat exchanger (used for chilled water production in the cooling mode of operation) is a brazed plate heat exchanger. A coil with wavy fins is used as the outdoor heat exchanger. The unit works following a flash tank vapor injection cycle (using a vapor-injected compressor). As shown in the figure, the liquid out of the condenser (coil) is expanded to an intermediate pressure through the expansion valve EEV-1 and directed to the flash tank. A fraction of the expanded refrigerant vaporizes and is injected into the intermediate vapor injection port of the compressor. The main part of the refrigerant out of the flash tank is in the liquid phase and flows to a second expansion valve, EEV-2, where it is expanded down to the evaporating pressure.

Water is used as the fluid media and is pumped from a 150 L tank to the heat pump's indoor heat exchanger (evaporator in figure 1). A variable speed pump is used in order to control the water flow rate to guarantee a water temperature variation of 5 K through the evaporator. The water supply temperature is controlled by adjusting the temperature level of the water tanks using an additional water circuit, valves and heat exchangers.

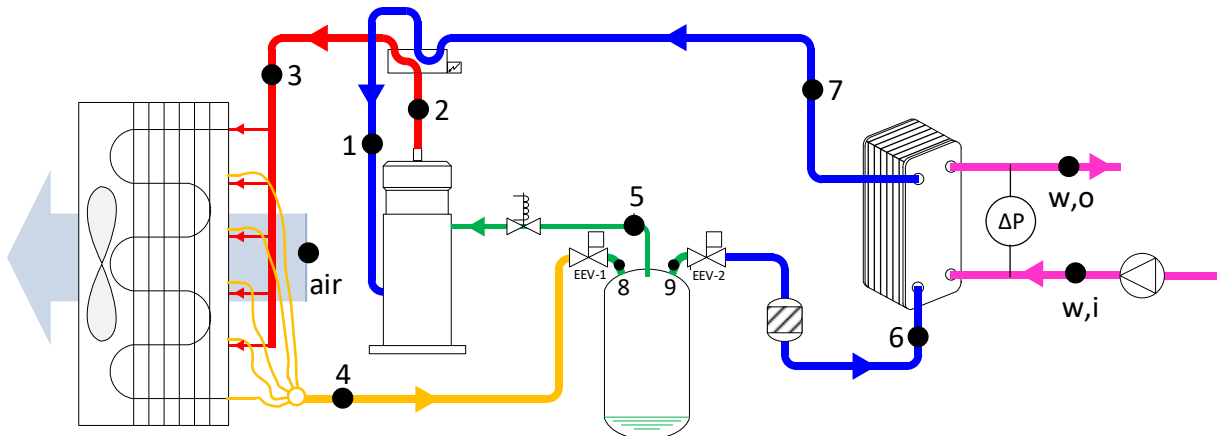


Figure 1: Schematic representation of the heat pump in the cooling mode of operation. (Numbers are related to refrigerant states at inlet/outlet of different components).

The heat pump is tested inside a climatic chamber which ambient conditions are controlled and changed according to the desired testing conditions. For the cooling mode of operation, only the temperature inside the climatic chamber needs to be controlled. An air sampling array consisting of 12 temperature sensors is used for measuring the dry-bulb temperature. The position and distribution of these sensors was done in accordance with AHRI Standard 551/591 (2018). To check for the recirculation of coil (condenser) discharged air back into the coil four additional temperature sensors were installed around the unit perimeter, as recommended in AHRI Standard 551/591 (2018).

The experimental facility has been equipped with a supervisory control and data acquisition (SCADA) system based on a PC and a programmable controller. Figure 1 shows the location of some relevant sensors used in the experimental setup and Table 1 summarize their main characteristics.

Table 1: Types of sensors and accuracies

Variable	Instrumentation	Accuracy
Water volumetric flow rate	Electromagnetic flow meter	$\pm 0.2\%$ reading
Water temperatures	PT 100 Class B 1/10	± 0.1 K
Water pressure drop	Differential pressure transducer	$\pm 0.1\%$ reading
Refrigerant temperatures	Digital sensors	± 0.5 K
Refrigerant pressure 1 (gauge)	Pressure transmitter	$\pm 1.2\%$ FS (-1 to 12.8 bar)
Refrigerant pressures 2-7 (gauge)	Pressure transmitter	$\pm 1.2\%$ FS (-1 to 45 bar)
Atmospheric pressure	Digital barometer	± 0.003 bar
Air dry-bulb temperatures	Digital sensors	± 0.1 K
Compressor electrical power	Power transducer	$\pm 0.2\%$ reading
Air fan electrical power	Power transducer	$\pm 0.5\%$ reading

3. TEST CONDITIONS AND EXPERIMENTAL PROCEDURE

Experiments were performed in the cooling mode of operation at different compressor and fan speed values. All tests were performed at A46W7 conditions (air at 46°C dry-bulb temperature and flow water at 7°C). The water flow rate was adjusted for a 5 K temperature variation through the indoor heat exchanger, i.e. 7°C flow and 12°C return water temperatures. Three different compressor speed values were tested (40%, 50% and 60% of maximum speed). For each compressor speed, the fan speed was varied from 55% to 95% of the maximum fan speed.

The heat pump unit controls the opening of the EEV-1 in order to adjust the intermediate pressure to the geometric mean of the condensation and evaporation pressures. The opening of the EEV-2 rules the degree of superheat at the

compressor inlet (slightly higher than at the evaporator outlet). During the experiments, the degree of superheat at the compressor inlet was nearly constant and equal to 11 ± 0.5 K.

All sensors were scanned within a time interval of 3 s. The SCADA system allows an automatic control of the water temperature entering the heat pump unit and the dry-bulb temperature of the climatic chamber. The water temperature at the outlet was also controlled automatically by means of a PID controller that regulates the water flow rate.

During each experiment, steady state conditions were confirmed by visualizing the measured variables in the SCADA system. In general, steady state operation was reached within a period of 1-2 hours. Thereafter, data recording during the next 40-60 minutes was performed for all the measured variables.

4. DATA REDUCTION AND ANALYSIS

From the measured data in the experimental setup, the thermodynamic conditions of the refrigerant, the water stream and the air stream are determined under steady state operating conditions. The thermodynamic conditions of the refrigerant at the inlet of the plate heat exchanger (evaporator) are determined from the conditions of the refrigerant at the inlet of the electronic expansion valve EEV-2 and assuming an isenthalpic process through the valve. All refrigerant and water properties were obtained using Refprop v.10 (Lemmon et al. 2018).

The following assumptions were considered in the thermal analysis of the heat pump:

1. Heat losses/gains in the refrigerant and water pipes are negligible (pipes are well insulated);
2. Heat transfer between the indoor heat exchanger and the surroundings is negligible;
3. Pressure drops in the refrigerant pipes between main components are negligible;
4. The process in an expansion valve is isenthalpic;
5. Saturated vapor leaves the flash tank (point 5) towards the compressor injection port;
6. Saturated liquid leaves the flash tank (point 9) towards the electronic expansion valve EEV-2.

The cooling power, the power input and the EER of the unit are calculated according to EN 14511:3: 2018. The effective power input is the sum of the power input for operation of the compressor, the power input for the fan, the portion of the water pump power required for the transport of the water flow through the heat pump unit, and all other auxiliary power requirements (this last contribution was neglected in this work, i.e. $\dot{W}_{aux} \approx 0$).

$$\dot{W}_{HP} = \dot{W}_{comp} + \dot{W}_f + \dot{W}_p + \dot{W}_{aux} \quad (1)$$

The indoor-side water pump is not an integral part of the heat pump. The effective power consumed by the pump is estimated using the following formula, based on the hydraulic power and the pump efficiency according to EN 14511:3: 2018.

$$\dot{W}_p = \dot{W}_{p,hyd} / \eta_p \quad (2)$$

The hydraulic power is determined from the measured water flow rate and the measured indoor-side static pressure difference,

$$\dot{W}_{p,hyd} = \dot{V}_w \Delta P_w \quad (3)$$

For the pump efficiency, the formula proposed by EN 14511:3: 2018 for pumps that are not an integral part of the heat pump unit was used.

$$\eta_p = \frac{0.35744 \dot{W}_{p,hyd}}{1.7 \dot{W}_{p,hyd} + 17(1 - e^{-0.3 \dot{W}_{p,hyd}})} \frac{0.49}{0.23} \quad (3)$$

The cooling capacity of the water-cooled flow in the evaporator is obtained from an energy balance on the water flow across the evaporator (indoor heat exchanger):

$$\dot{Q}_w = \dot{V}_w \rho_w c_{p,w} (T_{w,i} - T_{w,o}) \quad (4)$$

This capacity is corrected to include the power associated with the indoor-side water pump,

$$\dot{Q}_c = \dot{Q}_w - \dot{W}_p (1 - \eta_p) \quad (5)$$

The energy efficiency ratio (EER) is calculated from the effective cooling power and the total power input:

$$EER = \frac{\dot{Q}_c}{\dot{W}_{HP}} \quad (6)$$

5. RESULTS AND DISCUSSION

A set of 15 experiments were performed changing the compressor speed and the fan speed of the heat pump.

Figure 2 shows on a p-h diagram the refrigerant cycles for compressor speed values of 2800 and 4200 rev/min (40% and 60% of the maximum speed) and a constant fan speed of 825 rev/min (75% of the maximum value). When decreasing the compressor speed, the cooling power in the evaporator (indoor heat exchanger) decreases, so the temperature approach between the refrigerant and the water flows decreases, leading to a higher evaporating temperature and pressure. Following an analogous analysis, it is concluded that when decreasing the compressor speed, the condensing temperature and pressure also decrease, as confirmed in Figure 2. Because the fan speed is not changed in this analysis, the pressure variation effect is more noticeable in the condenser side; this leads to a decrease of the intermediate pressure.

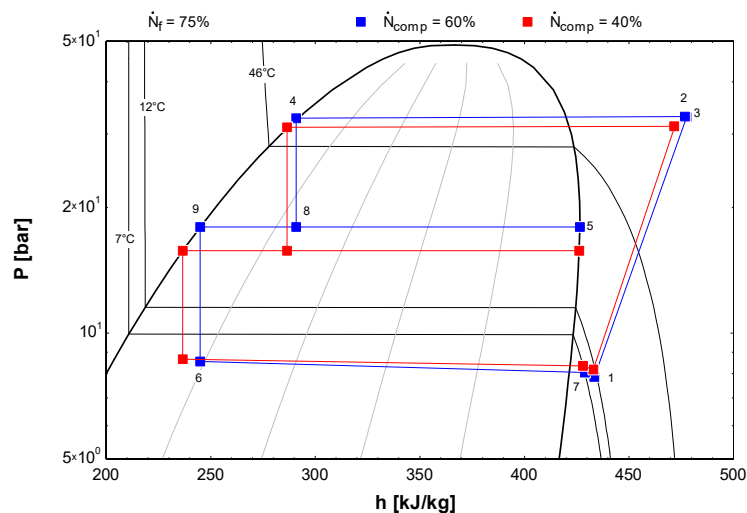


Figure 2: p-h diagrams of the refrigerant (R410A) cycles at two compressor speed values.

Figure 3 shows the refrigerant cycles when changing the fan speed at a constant compressor speed value. Now, the cooling and heating powers are expected to be somehow similar for the two fan speed values. As a result, not relevant changes are expected in the evaporating pressure, as confirmed in the results of Figure 3. However, when the fan speed is increased from 55% to 95% of its maximum value, the air-side temperature variation decreases and the air-side heat transfer coefficient increases, leading to a lower condensing temperature and pressure.

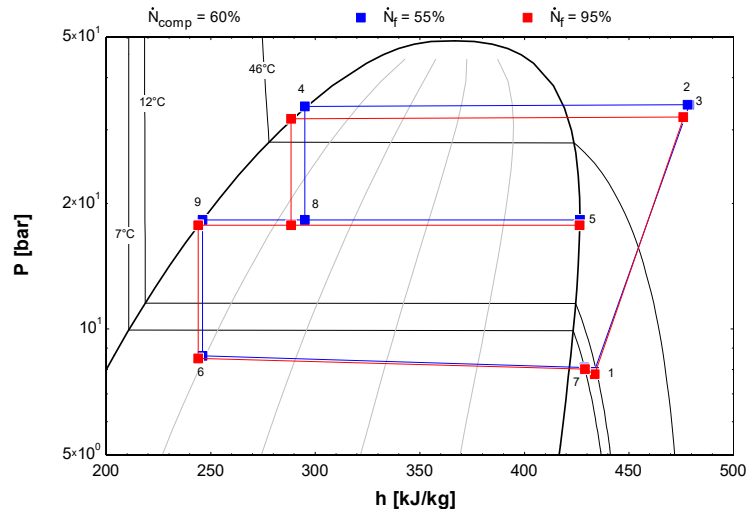


Figure 3: p-h diagrams of the refrigerant (R410A) cycles at two fan speed values.

Figure 4 shows the numerical results of the cooling power as a function of the fan speed for three different compressor speed values. As expected, the capacity increases with the compressor speed. However, for the range of values tested in this work, the capacity is not sensitive to the air fan speed.

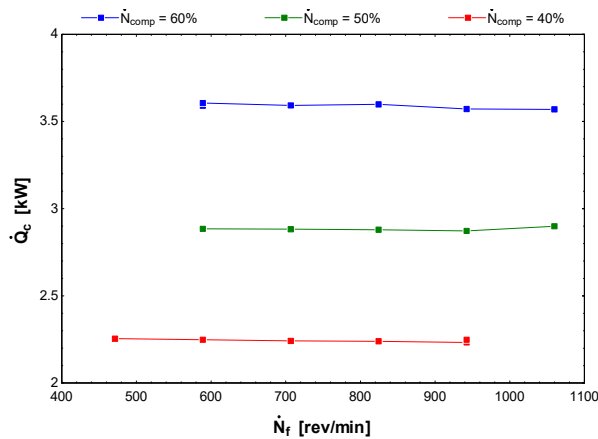


Figure 4: Cooling capacity as a function of the fan speed for three different compressor speed values.

Figure 5a) shows the closest approach temperature (CAT) in the condenser (coil) for the same experiments. As expected, the higher the compressor speed the higher the CAT in the coil. Increasing the fan speed leads to a more efficient heat transfer process and lower CAT values. Figure 5b) shows that the suction pressure increases slightly when reducing the compressor speed but it is somehow insensitive to the fan speed. However, the discharge pressure varies in harmony with the CAT evolution in the condenser; i.e. the discharge pressure decreases when decreasing the compressor speed and increasing the fan speed.

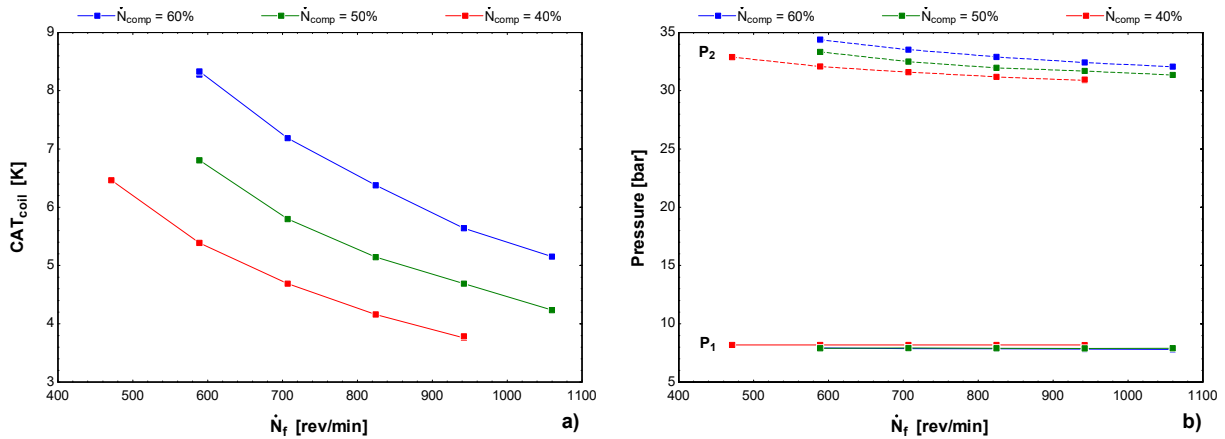


Figure 5: Effect of the fan speed for three different compressor speed values on a) the closest approach temperature in the condenser (coil) and b) the suction and discharge pressures

The compressor, air-fan and total heat pump input powers are represented in Figure 6. The compressor power decreases with its rotational speed. As shown before, the higher the fan speed, the lower is the discharge pressure leading to lower compressor powers. The figure also shows that the fan power increases monotonically with its speed, but it is not affected by the compressor speed. Numerical values shown in Figure 6a reflect that the fan powers are one order of magnitude lower than the compressor powers. Then, increasing the fan speed improves the heat transfer process in the condenser coil, leading to lower condensing pressures and compressor powers. At low fan speeds, the fan power increase is compensated by the decrease of the compressor power. However, at high fan-speed values, a further increase of the fan speed leads to a fan power increase that surpasses the compressor power reduction; as a result, the total input power also increases, as confirmed in Figure 6b. In summary, when increasing the fan speed, the total input power first decreases down to a minimum value, but then it increases with a further increase of the fan speed.

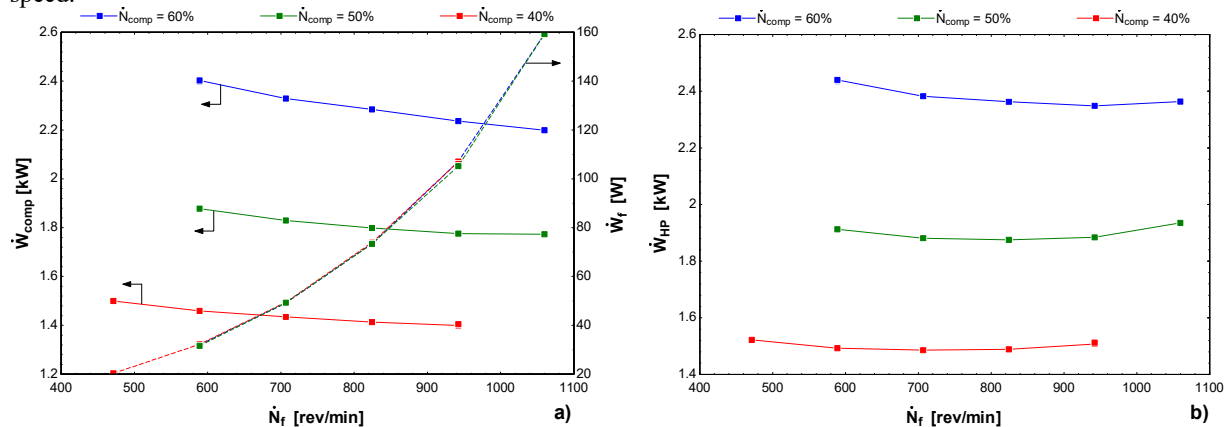


Figure 6: Effect of the fan speed for three different compressor speed values on a) the compressor and fan input powers, and b) the total heat pump input power. (Arrows below curves indicate the ordinate to use).

The results for the energy efficiency ratio (EER) are represented in Figure 7a). As shown previously in Figures 4 and 6, the cooling capacity is somehow insensitive to the fan speed, whereas for the total input power an optimum fan-speed that minimizes the total input power was found for each of the three compressor speeds tested. As a result, we should expect an optimum fan speed value that maximizes the EER, as confirmed in the numerical results of Figure 7a). Results also show that the lower the compressor speed (the cooling power) the lower is the optimum fan speed value. For the range of conditions tested, decreasing the fan speed from its highest value to the optimum one represented an EER improvement of 2% and 3% for the tests with the compressor running at 40% and 60% of its maximum rotational speed, respectively.

Figure 7b) shows results of some additional tests performed at A35W7 conditions. The trends are similar to the A46W7 tests, though the EER values are higher. Now the effect of the fan speed is greater than before, and can represent and improvement of up to 6%.

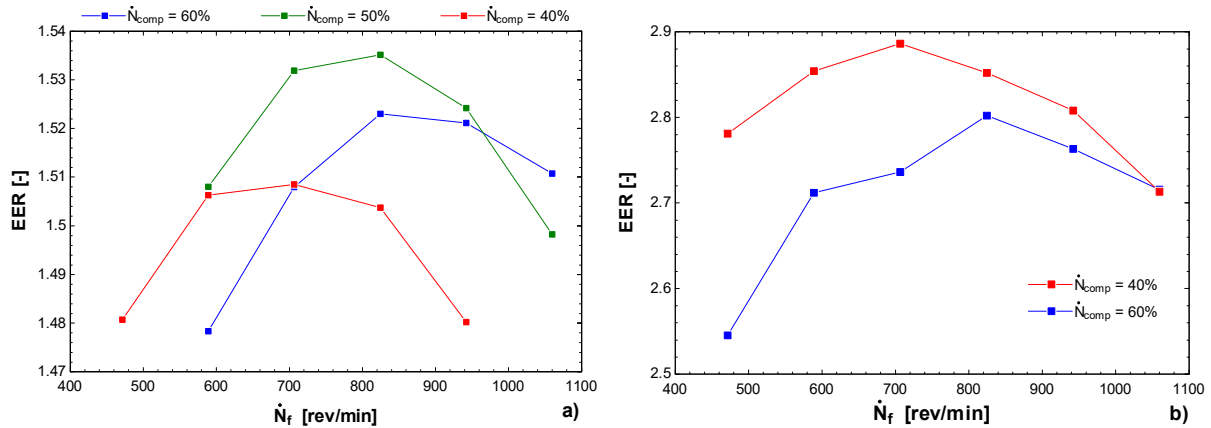


Figure 7: EER as a function of the fan speed for three different compressor speed values. Results at a) A46W7 and b) A35W7 conditions.

6. CONCLUSIONS

This paper presented an experimental study of the effect of the compressor and fan speeds on the performance of an air-to-water heat pump unit working in the cooling mode of operation. The refrigerant used was R410A. All tests were performed at A46W7 conditions. From the analysis of the experimental results, the following conclusions are obtained:

- Increasing the fan speed had a small effect on the cooling capacity, but it led to lower condensing pressures and lower compressor powers.
- When increasing the fan speed, the total input power of the unit first decreases down to a minimum value, but then it increases with a further increase of the fan speed.
- For each compressor speed tested, an optimum fan speed value that maximizes the EER could be found. The optimum fan speed decreases when the compressor speed (and as a result the cooling power) decrease.
- For the range of conditions tested in this work, the effect of the fan speed on the EER can represent an improvement of up to 6%.

NOMENCLATURE

CAT	closest approach temperature	(K)
COP	coefficient of performance	(-)
c_p	specific heat at constant pressure	(kJ/(kg·K))
EER	energy efficiency ratio	(-)
h	specific enthalpy	(kJ/kg)
\dot{N}	rotational speed	(rev/min)
P	pressure	(kPa, bar)
\dot{Q}	heat transfer rate	(kW)
SCOP	seasonal coefficient of performance	(-)
SEER	seasonal energy efficiency ratio	(-)
T	temperature	(°C)
\dot{V}	volumetric flow rate	(m ³ /s)
\dot{W}	power	(kW, W)

Greek letters

Δ	variation
η	efficiency

ρ density (kg/m³)

Subscript

aux	auxiliary
c	cooling
comp	compressor
f	fan
i	inlet
HP	heat pump
hyd	hydraulic
o	outlet
p	pump
w	water

REFERENCES

- Bertsch, S.S & Groll E.A. (2008). Two-stage air-source heat pump for residential heating and cooling applications in northern U.S. climates. *Int. J. Refrig.*, 31(7), 1282–1292.
- EHPA (2020). *European heat pump market and statistics – Report 2020*, EHPA, Brussels, Belgium.
- Lemmon, E.W., Bell, I.H., Huber, M.L. & McLinden, M.O. (2018). *NIST Standard Reference Database 23: Reference Fluid Thermodynamic and Transport Properties-REFPROP*, Version 10.0. National Institute of Standards and Technology, Standard Reference Data Program, Gaithersburg.
- Navarro, E., Redón, A., González-Macia, J., Martínez-Galvan, I.O. & Corberán J.M. (2013). Characterization of a vapor injection scroll compressor as a function of low, intermediate and high pressures and temperature conditions. *Int. J. Refrig.*, 36, 1821-1829.
- Redón, A., Navarro-Peri, E., Pitarch, M., González-Macia, J. & Corberán, J.M. (2014). Analysis and optimization of subcritical two-stage vapor injection heat pump systems. *App. Energy*, 124, 231-240.
- Shuxue, X., Guoyuan, M., Qi, L. & Zhongliang, L. (2013). Experiment study of an enhanced vapor injection refrigeration/heat pump system using R32. *Int. J. Therm. Sci.*, 68, 103-109.
- UNEP (2019). *Report of the refrigeration, air-conditioning and heat pumps technical options committee*. United Nations Environment Programme, Nairobi, Kenya.
- Wang, W. & Li, Y. (2019). Intermediate pressure optimization for two-stage air-source heat pump with flash tank cycle vapor injection via extremum seeking. *Appl. Energy*, 238, 612-616.
- Winandy, E. & Lebrun, J. (2002) Scroll compressors using gas and liquid injection: experimental analysis and modeling. *Int. J. Refrig.*, 25, 1143-1156.
- Xu, X., Hwang, Y. & Radermacher, R. (2011). Refrigerant injection for heat pumping/air conditioning systems: Literature review and challenges discussions. *Int. J. Refrig.*, 34, 402-415.

ACKNOWLEDGEMENT

The authors would like to acknowledge the Spanish ‘Agencia Estatal de Investigación’ for funding this work within the ‘Programa Estatal de I+D+i Orientada a los Retos de la Sociedad del Plan Estatal de Investigación Científica y Técnica y de Innovación 2017-2020’ (grant PID2019-104762RB-I00 / AEI / 10.13039/501100011033)